Cell Cycle Programs of Gene Expression Control Morphogenetic Protein Localization

Matthew Lord, Melody C. Yang, Michelle Mischke, and John Chant

Department of Molecular and Cellular Biology, Harvard University, Cambridge, Massachusetts 02138

Abstract. Genomic studies in yeast have revealed that one eighth of genes are cell cycle regulated in their expression. Almost without exception, the significance of cell cycle periodic gene expression has not been tested. Given that many such genes are critical to cellular morphogenesis, we wanted to examine the importance of periodic gene expression to this process. The expression profiles of two genes required for the axial pattern of cell division, *BUD3* and *BUD10/AXL2/SRO4*, are strongly cell cycle regulated. *BUD3* is expressed close to the onset of mitosis. *BUD10* is expressed in late G1. Through promotor-swap experiments, the expression profile of each gene was altered and the consequences examined. We found that an S/G2 pulse of *BUD3* expression controls the timing of Bud3p localization, but that this timing is not critical to Bud3p function. In contrast, a G1 pulse of *BUD10* expression plays a direct role in Bud10p localization and function. Bud10p, a membrane protein, relies on the polarized secretory machinery specific to G1 to be delivered to its proper location. Such a secretion-based targeting mechanism for membrane proteins provides cells with flexibility in remodeling their architecture or evolving new forms.

Key words: cell cycle • localization • secretory pathway • morphogenesis • budding yeast

Introduction

Genomic expression studies in budding yeast have suggested that coordinated cell cycle gene expression is critical to a wide variety of cellular processes (Cho et al., 1998; Chu et al., 1998; Spellman et al., 1998). However, experimental data directly testing this view is for the most part lacking. Many genes, whose expression is regulated by the cell cycle, are required for cell morphogenesis and polarization during cell division by budding. The potential exists that ordered periodic gene expression in the cell cycle is critical to morphogenesis. Here, we test this view by manipulating the expression profiles of two morphogenetic genes, *BUD3* and *BUD10*, both of which are involved in controlling spatial patterns of cell division.

Yeast cells become highly polarized and maintain their polarity as the bud emerges and grows. During this time, DNA is replicated and segregated. Once the bud has grown to roughly the size of its mother, cytokinesis occurs. Budding can occur in two spatial patterns. Haploid cells exhibit the axial budding pattern in which mother and daughter cells bud adjacent to their previous site of cell division (Freifelder, 1960; Hicks et al., 1977; Chant and Pringle, 1995). Diploid cells exhibit the bipolar budding pattern in which both mother and daughter bud at their poles with overlaying biases for one pole or the other (Freifelder, 1960; Hicks et al., 1977; Chant and Pringle, 1995).

The axial budding pattern has been shown to specifically require four genes: *BUD3*, *BUD4*, *AXL1*, and *BUD10*/*AXL2* (Chant and Herskowitz, 1991; Fujita et al., 1994; Halme et al., 1996; Roemer et al., 1996). Deletion of any of these genes in haploids results in a loss of axial budding in favor of bipolar budding (Fujita et al., 1994; Chant et al., 1995; Halme et al., 1996; Roemer et al., 1996; Sanders and Herskowitz, 1996). Apart from Axl1p, whose localization has not been reported, all of these factors localize to the mother–bud neck and form a double ring structure encircling the neck just before cytokinesis (Chant et al., 1995; Halme et al., 1996; Roemer et al., 1996; Sanders and Herskowitz, 1996). At cytokinesis, these double rings are split to endow each progeny cell with a single ring marking the previous site of attachment. It is thought that these rings act as a spatial memory designating the site of mother–bud attachment as the location for axial budding in the next cell cycle (Chant et al., 1995; Halme et al., 1996; Roemer et al., 1996; Sanders and Herskowitz, 1996).

A complementary set of genes (*BUD7*, *BUD8*, *BUD9*, *RAX1*, and *RAX2*) is required for maintenance of the bipolar budding pattern in diploids (Fujita et al., 1994; Zahner et al., 1996; Chen et al., 2000). The products of these genes likely comprise, at least in part, the cell surface landmarks used by the cell for the bipolar pattern of division.

Address correspondence to John Chant, Department of Molecular and Cellular Biology, Harvard University, 7 Divinity Avenue, Cambridge, MA 02138. Tel.: (617) 496-9003. Fax: (617) 495-0758. E-mail: chant@fas.harvard.edu

Table I. Yeast Strains

Strain	Relevant genotype	Source
JC1030	*MATα ura3 leu2 trp1*	Chant et al., 1995
JC1997	*MATα ura3 leu2 trp1 bud3::URA3*	This study
JC1293	*MATα ura3 leu2 trp1*	This study
JC1295	*MATα ura3 leu2 trp1 bud10::URA3*	Halme et al., 1996
JC1296	*MATa ura3 leu2 trp1 bud10::URA3*	Halme et al., 1996
JC1362	*MATa ura3 leu2 trp1 his3 ade2 cdc15-2ts*	Benton et al., 1997
JC2123	*MATα ura3 leu2 trp1 his3 ade2 bud3::URA3cdc15-2ts*	Segregant from JC1997 × JC1362
JC2133	*MATα ura3 leu2 trp1 his3 ade2 bud10::URA3cdc15-2ts*	Segregant from JC1295 × JC1362
EJY301	*MATα ura3 leu2 trp1 his3 lys2 CDC3-HA::HIS3*	Johnson and Blobel, 1999
JC29	*MATa1-50 ura3 trp1 his4 can1*	Lab strain collection
JC2312	*MATα/a1-50 ura3/ura3 leu2/LEU2 trp1/trp1 HIS4/his4 CAN1/can1 bud10::URA3/BUD10*	Hemizygote of JC1295 × JC29
JC2313	*MATα/a1-50 ura3/ura3 leu2/LEU2 trp1/trp1 HIS4/his4 CAN1/can1*	Hemizygote of JC1293 × JC29

A third class of genes (*BUD1/RSR1*, *BUD2,* and *BUD5*) is required for both the axial and bipolar budding patterns (Bender and Pringle, 1989; Chant and Herskowitz, 1991; Chant et al., 1991). The products of these genes, a Ras-like GTPase and its regulators, are thought to act on both axial and bipolar markers, coupling them with cellular components involved in generating an axis of polarity towards the incipient bud site (Chant and Herskowitz, 1991).

The timings of Bud3p and Bud10p localization to the mother–bud neck are not the same. Bud3p, a non-membrane protein, becomes detectable at the onset of mitosis, whereupon it localizes to the mother–bud neck (Chant et al., 1995). Bud10p, a membrane protein, is present throughout the cell cycle (Halme et al., 1996; Roemer et al., 1996). Bud10p localizes to the incipient bud site in G1 phase and then remains in the mother–bud neck as the bud grows outward (Halme et al., 1996; Roemer et al., 1996). Just before cytokinesis, both proteins localize as a double ring structure encircling the mother–bud neck (Chant et al., 1995; Halme et al., 1996; Roemer et al., 1996). Neither Bud3p nor Bud10p requires the other for localization to the mother–bud neck, though conversion of Bud10p localization from a loose concentration to tight double rings requires Bud3p (Halme et al., 1996).

We and others (Cho et al., 1998; Spellman et al., 1998) found that the expression profiles of *BUD3* and *BUD10* are cell cycle specific. To investigate the importance of periodic gene expression, the expression profiles of *BUD3* and *BUD10* were altered by promoter-swap experiments.

Materials and Methods

Strains, Plasmids, Growth Conditions, and Genetic Methods

Yeast strains and plasmids are described in Tables I and II. Standard yeast genetic procedures and media (Rose et al., 1990) were used, unless specified. For producing a *bud3* deletion, plasmid pJC15 (Chant et al., 1995) carrying the *bud3* deletion was linearized with BamHI and EcoRI and transformed into strain JC1030. Ura$^+$ transformants that exhibited the bipolar pattern were isolated.

Plasmid Construction

pJC16 (prom^{GAL1}-BUD3). An EcoRI/BamHI *GAL1* promoter fragment was liberated from pRS316-*GAL* (E. Bi, University of Pennsylvania Medical School, Philadelphia, PA). An isolate of *BUD3* in YCp50, p35-1 (Chant et al., 1995), was digested with BamHI and SalI to liberate the *BUD3* region. The linearized YCp50 was then digested with EcoRI. The *GAL1* promoter fragment and the *BUD3* fragment were then double ligated into the EcoRI/SalI YCp50 to yield *BUD3* under the control of the *GAL1* promoter.

pJC117 (prom^{MET3}-hemagglutinin [HA]-BUD3). A 700-bp *MET3* promoter region was amplified from JC1030 genomic DNA with *Pfu* polymerase (Stratagene) using primers: MET3promoter (prom)[1]-BamHI-5′ (5′-GCGCGCGGATCCAATACCCGTCAAGATAAGAG-3′) and MET3prom-HindIII-3′ (5′-GCGCGCAAGCTTGTTAATTATACTT-TATTCTTG-3′). The *MET3* promoter was ligated into pAD5 via the BamHI and HindIII sites of the primers, replacing the alcohol dehydrogenase promoter of pAD5. The *BUD3* sequence was PCR amplified with *Pfu* polymerase from p35-1, and the fragment was ligated into *MET3* promoter-containing pAD5 via SalI and SacI sites present in the vector and the primers. Primers were BUD3-SalI-5′ (5′-CTATGTCGACTATGGA-GAAAGACCTGTCGTC-3′) and BUD3-SacI-3′ (5′-GACTGAGCT-CTCCGATAATTCTCACAGG-3′).

pJC1869 (prom^{MET3}-BUD10-HA). 623 bp of the 5′ portion of the *BUD10* coding region were amplified from pJC246 with *Pfu* polymerase using the primers BUD10-KpnI-5′ (5′-CCCCCCGGTACCATGACA-CAGCTTCAGATTT-3′) and BUD10-AgeI-3′(5′-GAAAATCCTTCA-ATGTCTGTAGCG-3′). pJC246 was linearized by KpnI and AgeI, which resulted in excision of the *BUD10* promoter and 623 bp of the *BUD10* open reading frame up to the unique AgeI site. This linearized plasmid was gel purified and ligated with the 5′ *BUD10* PCR product that had been digested with KpnI and AgeI. The resulting construct (pJC255) contained *BUD10-HA* lacking the *BUD10* promoter. *BUD10-HA* was excised from pJC255 by digestion with KpnI and SpeI, gel purified, and ligated into KpnI/SpeI linearized pJC1830 to yield pJC1869 carrying *BUD10-HA* under the *MET3* promoter.

pJC256 and pJC257 (prom^{BUD3}-BUD10-HA). 600 bp of *BUD3* upstream sequence were amplified from p35-1 with *Pfu* polymerase using the primers *BUD3*prom-EcoRI-KpnI-5′ (5′-GGGGAATTCGGTACCCCG-GATCCTGTATTATATCCAGTAA-3′) and BUD3prom-EcoRI-KpnI-3′ (5′-GGGGAATTCGGTACCTGGTGAGGTGTAAATATACTC-TTT-3′). The PCR product was ligated into pBluescript via the EcoRI sites of the primers. Ligation products were digested with KpnI to liberate the *BUD3* promoter, which was ligated into the KpnI site of pJC255. Two resulting constructs (pJC256 and pJC257) were sequenced (Harvard Medical School, DNA Core Facility), and it was confirmed that the constructs carried *BUD10* under the *BUD3* promoter.

Overexpression of BUD3

The *BUD3*-overexpression construct (pJC16) and YCp50 (control vector) were transformed into EJY301. Ura$^+$ colonies carrying the plasmids were selected. Each transformant was grown overnight in Ura$^-$ glucose complete synthetic medium (CSM). The cultures were divided into two samples, harvested, washed twice, and resuspended in either Ura$^-$ glucose or Ura$^-$ galactose CSM for 24 h. Morphological analysis of cells was performed by counting normally dividing cells versus cells producing elongated buds. For each sample, 600 cells were scored. Visualization of Cdc3-HA in all samples was performed by immunofluorescence, as described below.

[1]*Abbreviations used in this paper:* CSM, complete synthetic medium; HA, hemagglutinin; prom, promoter; OD, optical density.

Table II. Plasmids

Plasmid	Description	Source
p35-1	Original isolate of *BUD3* in YCp50	Chant et al., 1995
pJC15	pUC119 carrying *BUD3* region with *BUD3* open reading frame deleted and replaced by *URA3*	Chant et al., 1995
pAD5	*LEU2*-containing, 2μ-containing vector with the ADH promoter upstream of a single *HA* sequence	Field et al., 1988
pJC117	*MET3* promoter–controlled *HA-BUD3* carried in pAD5	This study
p*GAL*	*GAL1* promoter in pRS316, a *URA3*-containing, low copy, centromeric plasmid	E. Bi
pJC16	*GAL1* promoter–controlled *BUD3* carried in YCp50	This study
pJC246	*BUD10-HA* carried in pRS314, a *TRP1*-containing, low copy, centromeric vector	Halme et al., 1996
pJC1830	*MET3* promoter carried in YCplac22, a *TRP1*-containing, low copy, centromeric vector	Epp and Chant, 1997
pJC1869	*MET3* promoter–controlled *BUD10-HA* carried in pJC1830	This study
pJC256, 257	*BUD3* promoter–controlled *BUD10-HA* carried in pRS314	This study

Preparation of RNA Samples from Synchronized Cell Cultures

JC1362 (containing wild-type copies of *BUD3* and *BUD10*) in rich medium, JC2123 carrying pJC117 (prom^{MET3}-*BUD3*) in Leu$^-$Met$^-$ CSM, JC2133 carrying pJC256 (prom^{BUD3}-*BUD10*) in Trp$^-$ CSM, and JC2133 carrying pJC1869 (prom^{MET3}-*BUD10*) in Trp$^-$ Met$^-$ CSM were grown up overnight in 500-ml cultures at 25°C. When cultures reached an optical density at 600 nm (OD_{600}) of ~0.15, they were harvested and resuspended in 500 ml of their respective growth media that had been prewarmed to 37°C. *cdc15-2^{ts}*–based arrest was attained by incubation of cultures at 37°C for 4.5 h. Arrest was confirmed microscopically and cells were chilled on ice for 5–10 min before resumption of growth at 25°C (0 min after release from arrest). Samples (25 ml) were harvested every 15 min (for JC1362) or 30 min (for all others), frozen in liquid nitrogen, and stored at −80°C at time points from 0–240 min after arrest. These 25-ml samples were used for subsequent RNA sample preparation. The Hot Phenol Method of total RNA preparation (Köhrer and Domdey, 1991) was used. In addition, at every time point, 1 ml of culture was fixed in 4% formaldehyde for 30 min at 30°C. These samples were used to determine the budding index (the number of budded cells versus unbudded cells). For the initial portions of the synchronizations (60 min for Figs. 1, 3, and 4, and 90 min for Figs. 2 and 6) a modification of this basic method was used. Cells were scored as small budded versus other, due to the fact that cells recovering from the *cdc15-2* block are delayed in completing cell separation. Cultures synchronized in identical fashion were used to correlate budding index with spindle morphology.

Northern Blotting

Standard methods were employed (Sambrook et al., 1989) with the following modifications. 5 μl of RNA samples were mixed with 10 μl of RNA loading buffer (Ambion) and run on 1% agarose-MOPS gels containing 6% formaldehyde. Running buffer was 1× MOPS. Gels were washed five times in 0.1% diethyl pyrocarbonate–treated water then by a 45-min equilibration in 20× SSC. RNA was subjected to capillary transfer overnight onto Zeta Probe (Bio-Rad Laboratories) nylon membranes. Membranes were washed for 5 min in 6× SSC and dried at room temperature for 30 min on paper towels before baking them in a vacuum oven at 80°C for 1.5 h. Membranes were prehybridized for 1 h in UltraHyb (Ambion) at 55°C then hydridized overnight at 55°C with the appropriate radioactively labeled probes. 0.5–1.5 kb of *BUD3*, *BUD10*, *LEU2*, or *ACT1* were PCR amplified, gel purified, and used as templates for the manufacture of probes through the use of the "Prime-a Gene" Labeling System (Promega). After hybridization, membranes were washed twice at 55°C for 15 min in 2× SSC/0.1% SDS, and then by two washes for 30 min in 0.1× SSC/0.1% SDS. Blots were exposed to a BAS-III Imaging Plate (Fuji) for appropriate times. The Imaging Plate was processed by a Fujix BAS 2000 Imager (Fuji). Images were analyzed by MacBAS V2.5 (Fuji). Blots were stripped for reprobing by washing three times for 20 min in 0.1× SSC/0.5% SDS at 95°C.

Immunofluorescence and Calcofluor Staining

JC1997 carrying pJC117 (prom^{MET3}-*BUD3*) was grown overnight in Leu$^-$ Met$^-$ CSM. JC1296 carrying pJC246 (prom^{BUD10}-*BUD10*) or pJC256 (prom^{BUD3}-*BUD10*) was grown in Trp$^-$ CSM overnight. JC1296 carrying pJC1869 (prom^{MET3}-*BUD10*) was grown in Trp$^-$ Met$^-$ CSM overnight. At an OD_{600} of 0.3–0.5, cells were fixed in 4% formaldehyde at 30°C for 30–60 min and washed three times in PBS. Indirect immunofluorescence was performed as described by Pringle et al. (1991). A mouse anti-HA epitope monoclonal antibody (Jackson ImmunoResearch Laboratories) or rabbit anti-Bud3p antibody (Chant et al., 1995) was used to visualize the two proteins. The secondary antibodies used were CY3-conjugated goat anti–mouse IgG and FITC-conjugated goat anti–rabbit IgG (Jackson ImmunoResearch Laboratories). Microtubule staining was performed as described in Chant et al. (1995). Budding patterns were scored by staining bud scars with Calcofluor and observing with fluorescence microscopy (Pringle, 1991); 200–300 cells were scored for each set of counts. Fluorescence microscopy was performed using a Nikon Microphot SA microscope with a 63× Plan-apo objective.

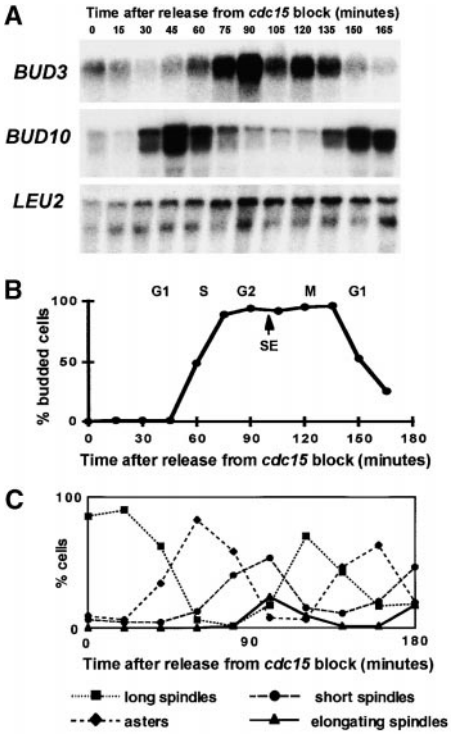

Figure 1. Cell cycle expression profiles of *BUD3* and *BUD10.* (A) Northern blot of *BUD3* and *BUD10* expression during the cell cycle of wild-type cells (JC1362). Synchronization of the cell cycle was achieved through use of a *cdc15-2^{ts}* background (Benton et al., 1997). *LEU2* is a cell cycle–constitutive control. (B) Cell cycle stages of the synchronized culture defined by the budding index (scored by counting unbudded versus budded cells; see Materials and Methods for details). SE denotes the initiation of spindle elongation. (C) Cell cycle stages of the synchronized culture were scored by microtubule morphologies.

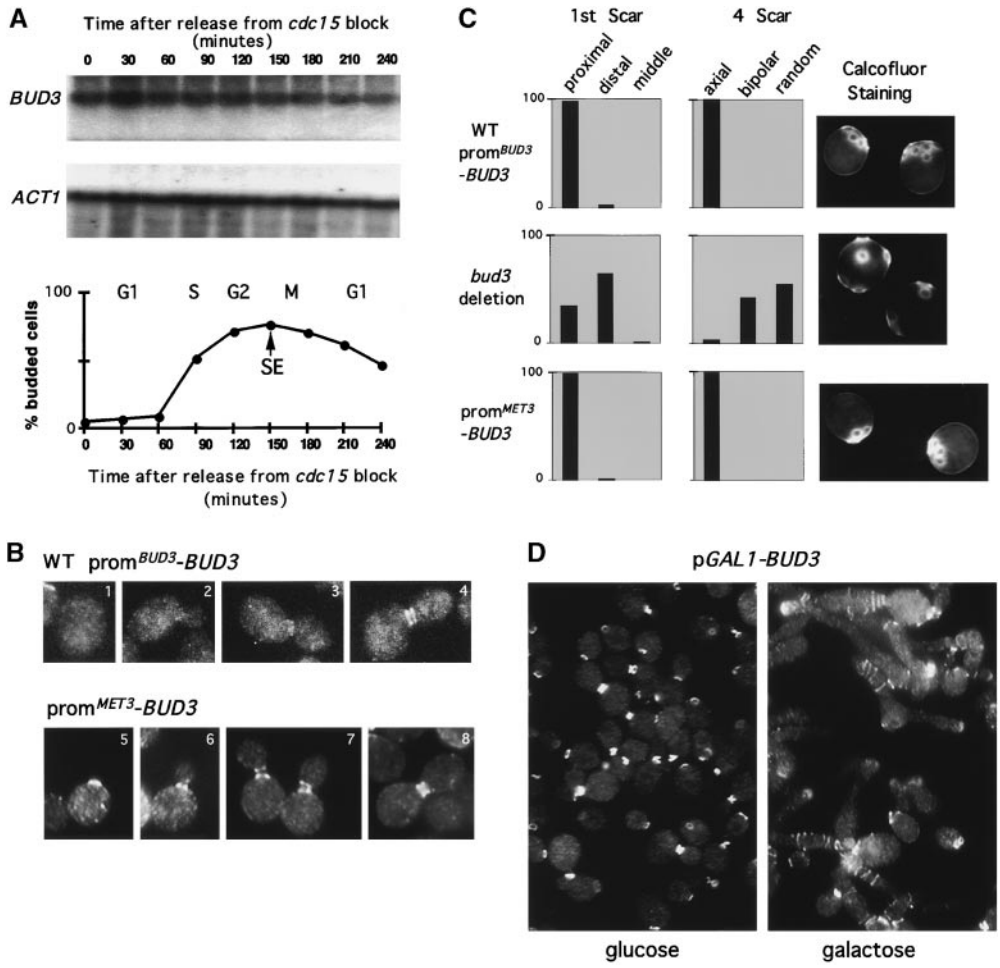

Figure 2. Cell cycle–constitutive expression of *BUD3*. (A) Northern blot analysis of *BUD3* expression in JC2123 carrying pJC117 (prom^{MET3}-*BUD3*). The graph depicts the cell cycle stages of the synchronized culture as defined by the budding index and spindle elongation (SE). *ACT1* is a cell cycle–constitutive control. (B) Localization of Bud3p during the cell cycle. The top images (1–4) show localization of Bud3p in strain JC1030 (anti-Bud3p antibody). The bottom images (5–8) show localization of HA-tagged Bud3p in JC1997 carrying pJC117 (prom^{MET3}-*BUD3*) under inducing conditions. (C) The ability of constitutively expressed *BUD3* to support axial budding. Bud scar counts are shown for wild-type cells (JC1030), *bud3*-deletion cells (JC1997), and constitutive *BUD3* cells (JC1997) carrying pJC117. For each, the arrangements of scars on cells with one bud scar and cells with four bud scars were scored relative to the birth scar after staining with calcofluor (Chant and Pringle, 1995). (D) Examples of cells exhibiting defects in morphology and septin (Cdc3p) localization upon overexpression of *BUD3*. EJY301 carrying the prom^{GAL1}-*BUD3* overexpression construct (pJC16) was grown in glucose-containing (repressing) or galactose-containing (inducing) media.

Western Blot Analysis

15 OD_{600} units of cells were harvested and washed with distilled water. Cells were resuspended in 150 μl lysis buffer (1% SDS, 2 mM PMSF plus protease inhibitors) and lysed with glass beads by vortexing on ice for a total of 6 min. 100 μl of lysis buffer was added to the extracts that were then centrifuged at 500 *g* for 2 min. Lysates were decanted and stored at −80°C if they were not required immediately. The protein concentrations of the lysates were determined using Pierce Coomassie Plus protein reagent (Pierce Chemical Co.). Equal protein levels from each lysate were loaded onto an SDS-PAGE gel and immunoblotted by standard methods (Sambrook et al., 1989). Mouse anti-HA epitope monoclonal primary antibodies (Jackson ImmunoResearch Laboratories) were used at a dilution of 1:500. Secondary antibodies were goat anti–mouse antibodies conjugated to horseradish peroxidase (Sigma–Aldrich) used at a dilution of 1:2,500. Blots were developed using the ECL Western blotting detection system (Amersham Pharmacia Biotech). Autoradiographs were scanned and the protein bands were quantitated using the MacBAS V2.5 program.

Pulsed Expression Experiments

Unsynchronized Cells. JC1296 carrying pJC1869 (prom^{MET3}-*BUD10*) was grown in repressing conditions (4 mM methionine, Trp^- CSM) overnight. At an OD_{600} of ~0.25, cells were spun down and washed three times in inducing medium (Trp^- Met^- CSM), and followed by a 30 min incubation in the same medium. Induction of *BUD10* expression was terminated by the addition of 4 mM methionine. Samples were harvested and fixed in formaldehyde (as described above) at 0, 60, and 120 min after cells were removed from inducing conditions. All samples were washed three times in PBS. Samples were subjected to analysis by immunofluorescence, as described above. Typically, 100 cells were scored per sample.

Synchronized Cells. JC2133 carrying pJC1869 (prom^{MET3}-*BUD10*) was grown up at 25°C in repressing conditions (4 mM methionine, Trp^- CSM) overnight. Cell synchronization was achieved as described earlier using the *cdc15-2*^{ts} mutation. The synchronized culture was divided in two: one half for late G1 induction and the other half for S/G2 induction. All subsequent incubations were performed at 25°C. 35 min after release from cell cycle arrest, late G1 induction was performed by the following method: cells were washed three times in inducing medium (Trp^- Met^- CSM) and incubated 45 min in the same medium. Induction was terminated by addition of 4 mM methionine and an additional brief incubation. At 90 min after release from arrest, cell samples were taken and fixed (as performed above). Cells were washed three times in PBS and subjected to analysis by immunofluorescence. S/G2 induction was performed in identical fashion, but 110 min after release from cell cycle arrest.

Results

BUD3 and BUD10 Expression Are Cell Cycle Regulated

Microarray experiments indicated that the expression profiles of the axial budding–specific genes, *BUD3* and *BUD10*, are tightly cell cycle regulated, being expressed in S/G2 and late G1, respectively (Cho et al., 1998; Spellman et al., 1998). We confirmed this observation by Northern

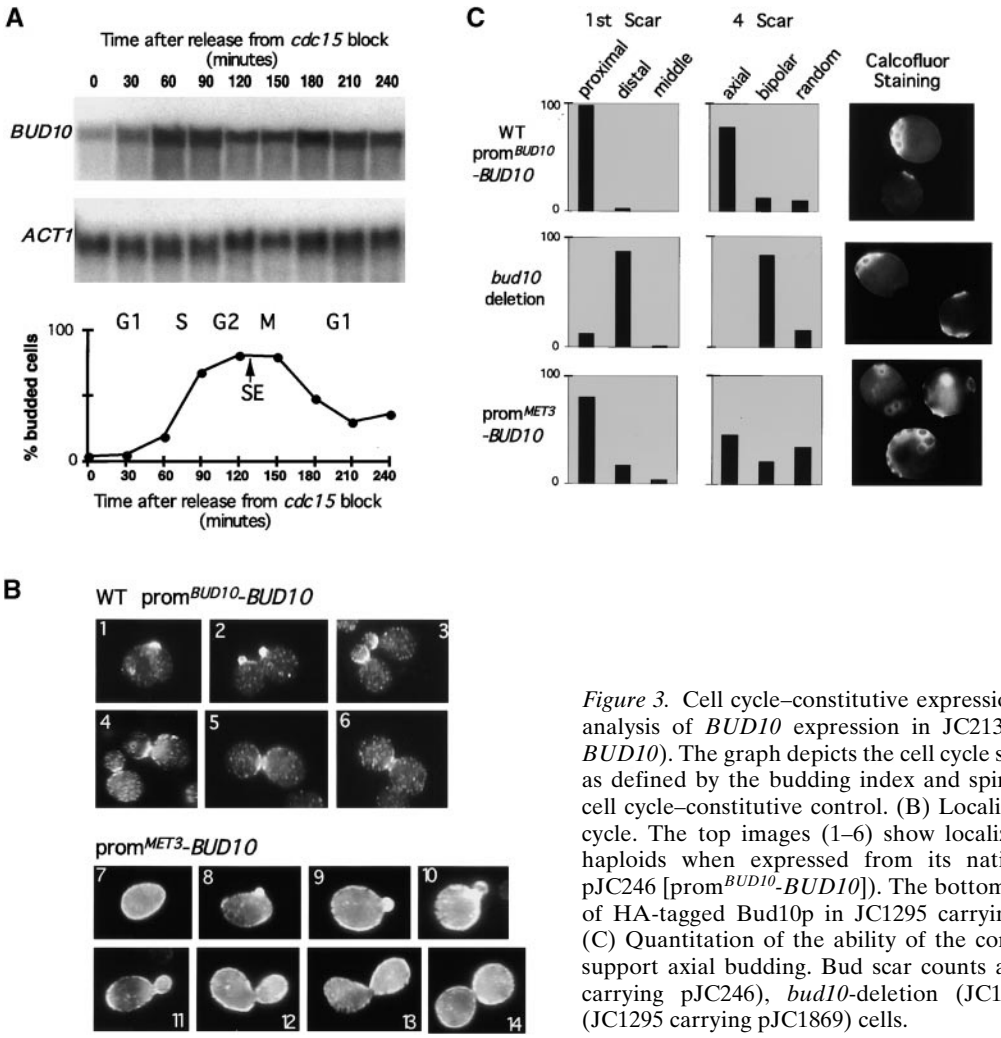

Figure 3. Cell cycle–constitutive expression of *BUD10.* (A) Northern blot analysis of *BUD10* expression in JC2133 carrying pJC1869 (prom^{MET3}-*BUD10*). The graph depicts the cell cycle stages of the synchronized culture as defined by the budding index and spindle elongation (SE). *ACT1* is a cell cycle–constitutive control. (B) Localization of Bud10p during the cell cycle. The top images (1–6) show localization of HA-tagged Bud10p in haploids when expressed from its native promoter (JC1295 carrying pJC246 [prom^{BUD10}-*BUD10*]). The bottom images (7–14) show localization of HA-tagged Bud10p in JC1295 carrying pJC1869 (prom^{MET3}-*BUD10*). (C) Quantitation of the ability of the constitutively expressed *BUD10* to support axial budding. Bud scar counts are shown for wild-type (JC1295 carrying pJC246), *bud10*-deletion (JC1295), and constitutive *BUD10* (JC1295 carrying pJC1869) cells.

blot analysis. *BUD3* mRNA levels peaked after bud emergence at the S/G2 phase of the cell cycle (Fig. 1, A and B). *BUD10* mRNA levels peaked at the start of the cell cycle just before bud emergence in late G1 phase (Fig. 1, A and B). Both budding index (Fig. 1 B) and an assessment of microtubule morphology (Fig. 1 C) confirmed that this method of synchronization was effective.

Constitutive Expression of BUD3 Does Not Affect Its Localization or Function

The importance of a pulse of *BUD3* expression at the S/G2 phase of the cell cycle was tested by expressing *BUD3* from the *MET3* promoter under steady state inducing conditions (methionine-deficient medium). Northern blot analysis of *BUD3* confirmed that *BUD3* expression was now uniform throughout the cell cycle (Fig. 2 A). Immunofluorescence was employed to analyze Bud3p localization (Fig. 2 B). Bud3p was able to localize to the mother–bud neck as observed in the wild-type situation. However, the normal temporal regulation of Bud3p localization was lost. In wild-type cells, Bud3p localizes to the mother–bud neck coincident with the onset of mitosis (Fig. 2 B, cells 1–4). In the constitutive strain, Bud3p localized to the mother–bud neck at all phases of the cell cycle (Fig. 2 B, cells 5–8). Premature Bud3p localization had little consequence on Bud3p function: constitutive expression of *BUD3* under the *MET3* promoter complemented a *bud3* null mutation for the axial pattern (Fig. 2 C). Thus, the periodic expression of *BUD3* during the cell cycle is the basis for the tight temporal control of Bud3p localization, but this control is not critical for Bud3p function.

Possible Morphogenetic Consequences of BUD3 Misexpression

To further test the consequence of altered *BUD3* expression, we overexpressed *BUD3* throughout the cell cycle by using a *GAL1* promoter–*BUD3* construct. Galactose-induced overexpression of *BUD3* resulted in a cell division defect in 42% of cells (Fig. 2 D): cells failed to divide correctly and displayed large, elongated buds, a defect similar to that of mutants defective in the septins (Longtine et al., 1996). Immunofluorescence was employed to analyze the consequences of *BUD3* overexpression on the localization of the septin Cdc3p. In glucose medium, cells exhibited wild-type Cdc3p localization as rings present at division sites (Fig. 2 D). In galactose medium, many cells displayed aberrant Cdc3p localization (Fig. 2 D), which was visible as multiple rings found throughout elongated buds or as a patch at the tips of elongated buds. Upon closer examination of the strain carrying the prom^{MET3}-*BUD3* construct,

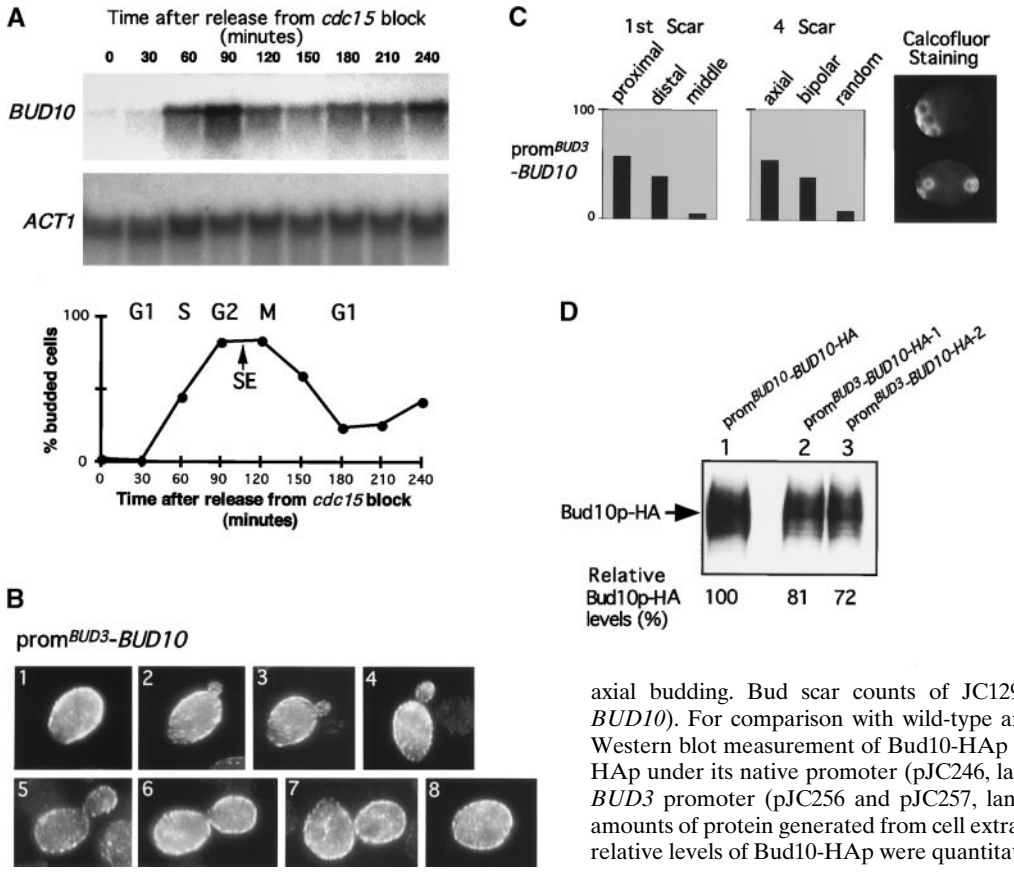

Figure 4. Expression of *BUD10* from the *BUD3* promoter. (A) Northern blot analysis of *BUD10* expression in JC2133 carrying pJC256 (prom^{BUD3}-*BUD10*). The graph depicts the cell cycle stages of the synchronized culture as defined by the budding index and spindle elongation (SE). *ACT1* is a cell cycle–constitutive control. (B) Localization of Bud10p during the cell cycle. The images (1–8) show the localization of HA-tagged Bud10p in JC1295 carrying pJC256 (prom^{BUD3}-*BUD10*). For comparison with the localization of Bud10p in wild-type cells, see Fig. 3 B. (C) Quantitation of the ability of the construct containing *BUD10* under the control of the *BUD3* promoter to support axial budding. Bud scar counts of JC1295 carrying pJC256 (prom^{BUD3}-*BUD10*). For comparison with wild-type and *bud10* cells see Fig. 3 C. (D) Western blot measurement of Bud10-HAp levels in JC1295 carrying Bud10-HAp under its native promoter (pJC246, lane 1) or under the control of the *BUD3* promoter (pJC256 and pJC257, lanes 2 and 3, respectively). Equal amounts of protein generated from cell extracts were loaded in each lane, and relative levels of Bud10-HAp were quantitated (see Materials and Methods).

we were able to observe a similar morphological defect in a minority of cells (3 versus 0% in wild-type cells). Thus, inappropriate expression of *BUD3* can have deleterious consequences (see Discussion).

Constitutive or Delayed Periodic Expression Affects Bud10p Localization and Function

The importance of temporally regulated *BUD10* expression in late G1 phase was tested by two perturbations: expression from the constitutive *MET3* promoter and expression from the periodic *BUD3* promoter. *BUD10* expression under the *MET3* promoter appeared to occur uniformly throughout the cell cycle, barring an initial lag at 0 and 30 min after release from arrest (Fig. 3 A). The initial low levels of *BUD10* expression, which quickly recovered, were likely a consequence of cells exiting from the *cdc15-2*^{ts}–based arrest. Immunofluorescence was undertaken to investigate whether constitutive expression of *BUD10* affected Bud10p localization. Constitutive *BUD10* expression resulted in uniform distribution of Bud10p throughout the plasma membrane at all points in the cell cycle (Fig. 3 B). In rare instances, Bud10p was found somewhat concentrated in small buds (Fig. 3 B, 8 and 9). This effect can be accounted for if we consider the fact that during constitutive expression, some *BUD10* is still expressed at the normal time at late G1. Expression at this point in the cell cycle apparently allows Bud10p to occasionally concentrate at small buds. The uniform localization of Bud10p resulting from constitutive expression affected the axial pattern of budding (Fig. 3 C). First bud-scar analysis revealed a small reduction in the number of cells budding at the proximal pole (80 versus 86% in wild-type cells) (Fig. 3 C). Four bud-scar analysis portrayed a larger effect: only 45% of cells budded in an axial manner as compared with 78% in the wild-type control (Fig. 3 C). The levels of Bud10p in wild-type cells and cells expressing *BUD10* from the *MET3* promoter were compared by Western blot analysis: approximately sevenfold more Bud10p was produced via the constitutive *MET3* promoter than via the native promoter in wild-type cells (results not shown). However, it seemed unlikely that the defects in the axial budding pattern apparent in cells expressing *BUD10* constitutively were due to excessive levels of Bud10p causing interference: expression of *BUD10* from the *MET3* promoter plasmid was recessive in a wild-type haploid (JC1293) background (results not shown).

In a second set of experiments, *BUD10* expression was delayed until S/G2 by placing *BUD10* under control of the *BUD3* promoter. The pulsatile nature of *BUD10* expression was preserved, but its timing was altered. Northern blot analysis confirmed that expression of *BUD10* from the *BUD3* promoter occurred in a pulse that was delayed to the S/G2 phase of the cell cycle (Fig. 4 A). Just as with constitutive expression, delayed expression resulted in a uniform distribution of Bud10p throughout the plasma membrane (Fig. 4 B). Expression of *BUD10* under the *BUD3* promoter in haploids resulted in a similar defect in the axial pattern as observed when *BUD10* was placed under the *MET3* promoter. Only 57% of cells exhibited proximal bud-site selection (versus 86% of wildtype haploids) (Fig. 3 C) on the basis of first bud-scar analysis (Fig.

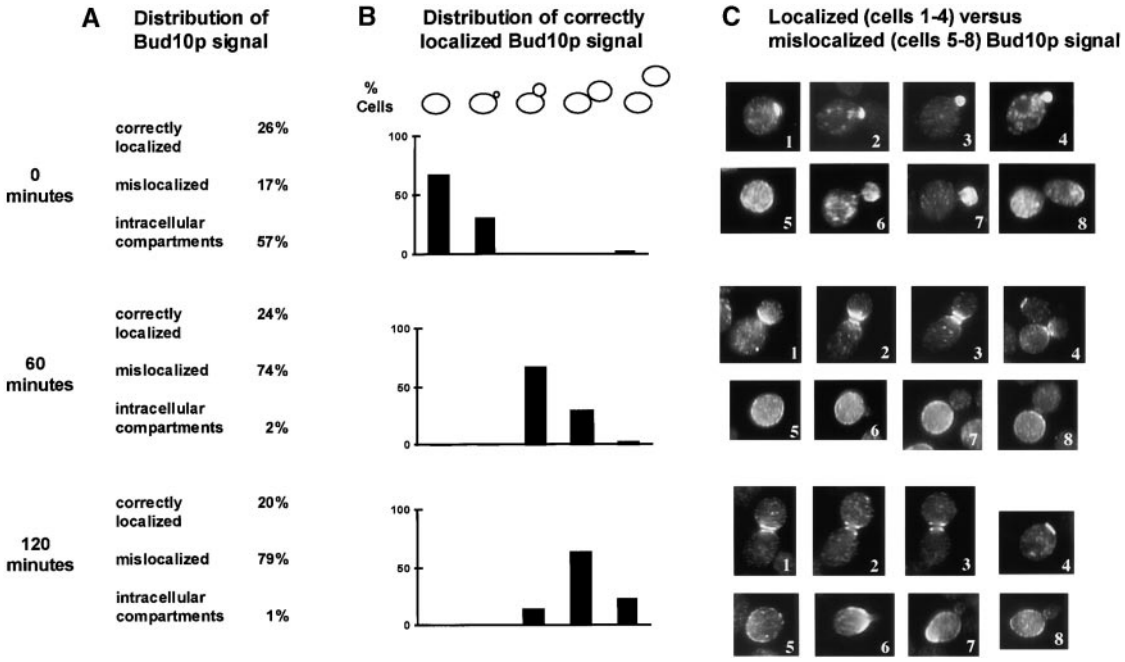

Figure 5. Pulsing *BUD10* expression in an asynchronous culture. (A) Quantitation of the distribution of HA-tagged Bud10p signal in JC1296 carrying pJC1869 (prom^{MET3}-*BUD10*). At each time point after pulsing of *BUD10* expression from the *MET3* promoter (0, 60, and 120 min), the distribution of Bud10p signal was placed into three categories: correctly localized, mislocalized, and intracellular. (B) Position in the cell cycle at which a correctly localized HA-tagged Bud10p signal was apparent by immunofluorescence analysis. (C) Immunofluorescence analysis of HA-tagged Bud10p after a brief induction of *BUD10-HA* expression. At each time point after induction, examples of correctly localized Bud10p (cells 1–4) and incorrectly localized Bud10p signals (cells 5–8) are shown.

4 C). On four bud-scar analysis, only 54% of cells budded in an axial manner as compared with 78% in the wild-type control (Figs. 4 C and 3 C). As observed above for the prom^{MET3}-*BUD10* construct the prom^{BUD3}-*BUD10* construct was recessive in its effects (results not shown). To eliminate the possibility that a significantly altered level of Bud10p expression from the *BUD3* promoter was the basis for the defects in its localization, Western blot analysis was performed. As shown in Fig. 4 D, expression of *BUD10* under the *BUD3* promoter resulted in levels of Bud10p very similar (72–81%) to the levels apparent in wild-type cells. The possibility remained that reduction in Bud10p levels generated the defects reported above. Therefore, we examined the budding pattern of a heterozygous α/a1 *BUD10/bud10* strain (JC2312), which behaves as an α cell. This strain, which in principle expresses 50% the normal levels of Bud10p, exhibited a wild-type axial budding pattern identical to that of the wild-type control, JC2313 (results not shown). Therefore, the quantity of Bud10p produced from the *BUD3* promoter appeared sufficient for carrying out its function. Based on these two promoter-swap experiments, we conclude that a G1 pulse of *BUD10* expression is critical to Bud10p localization and function.

Pulsed Expression of BUD10 in Late G1 Phase Restores Correct Localization of Bud10p

The experiments above suggest that a cell cycle–specific temporal pulse of *BUD10* expression is critical to Bud10p localization. According to this view, it should be possible to restore Bud10p localization by artificially producing a pulse of *BUD10* expression in G1. Through use of the construct in which *BUD10* was under the control of the *MET3* promoter, pulsed *BUD10* expression could be produced by transferring cells grown in medium with methionine (repressing) to a brief incubation in methionine-deficient medium (inducing). Optimization indicated that a pulse of 30 min in methionine-deficient medium was sufficient to stimulate detectable Bud10p in 20–25% of cells (results not shown). 30 min is a relatively short pulse as the cell cycle time is ~150 min in this medium at 30°C. Induction experiments were performed on unsynchronized or synchronized cell cultures.

The unsynchronized experiment was performed as follows. A log phase cell culture was induced for 30 min of *BUD10* expression. Samples were taken immediately, 60 and 120 min after induction was completed. Most of the cells analyzed at the three different time points exhibited uniform localization of Bud10p, rather than the tight bud site and mother–bud neck localizations seen in wild-type cells (Fig. 5, A and C, cells 5–8, all three time points). Considering the previous set of experiments, mislocalization in most cells was presumably due to expression having occurred at the wrong time in the cell cycle, i.e., at a time other than late G1 phase. A fraction of cells (20–26%) did display correct localization of Bud10p. Localization was scored as correct if it appeared as expected for a wild-type cell at the corresponding phase of the cell cycle. Correct Bud10p localization was presumably a result of a pulse of expression having occurred in those cells traversing G1 when induction occurred (Fig. 5, A and C, cells 1–4 at 0, 60, and 120 min). Correctly localized Bud10p signal was examined at 0, 60, and 120 min after induction and divided into five subcategories based on the cell cycle stage at

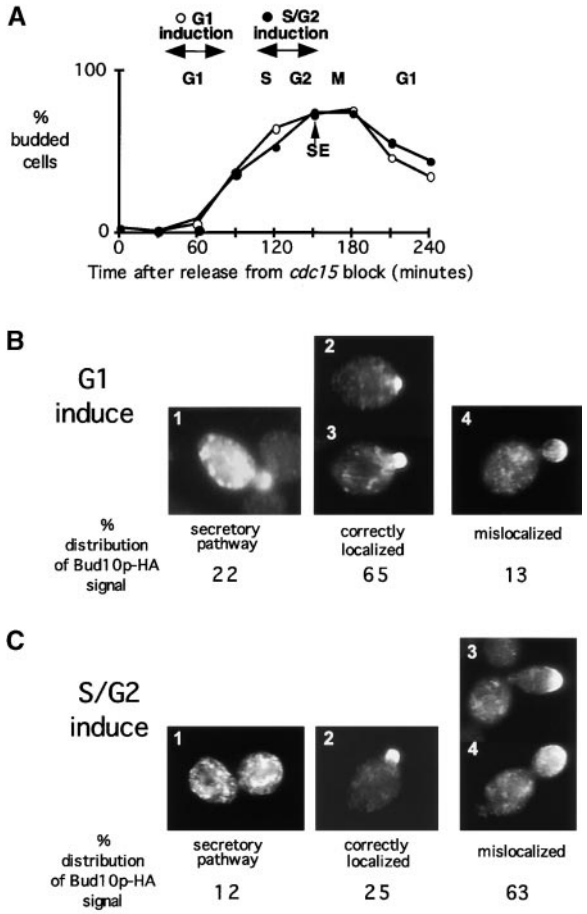

Figure 6. Pulsing *BUD10* expression in synchronous cultures. (A) The graph depicts synchrony profiles of JC2133 cultures carrying pJC1869 (prom^{MET3}-*BUD10*), which were pulsed for *BUD10* expression. The cell cycle stage was defined by the budding index and spindle elongation (SE). Late G1 and S/G2 inductions of *BUD10* expression were achieved by a 45-min incubation of cell samples in methionine-deficient medium for the periods indicated with double headed arrows. Under these conditions, the cell cycle length (cell doubling time) was ~210 min. (B) The percent distribution of Bud10-HAp signal found in the secretory pathway, correctly localized or mislocalized, was scored after induction centered on late G1 phase. Examples of each type of localization are shown above the values: cell 1, secretory pathway localization; cells 2 and 3, correctly localized; and cell 4, mislocalized signal. (C) The percent distribution of Bud10-HAp signal found in the secretory pathway, correctly localized or mislocalized in the cell, was scored after induction centered on S/G2 phase. Examples of each type of localization, as detected by immunofluorescence, are shown above the values: cell 1, secretory pathway localization; cell 2, correctly localized; and cells 3 and 4, mislocalized signal.

which the correctly localized signal was seen (Fig. 5 B). A correlation was apparent between the time after induction and the point in the cell cycle at which Bud10p was observed to be correctly localized. At 0 min after induction, correctly localized Bud10p signal was mostly concentrated at incipient bud sites or in small buds (Fig. 5, B and C, cells 1–4); 60 min after induction, a majority of the correctly localized signal was evident at the bases of medium-sized buds (Fig. 5, B and C, cells 1–4); 120 min after induction, most of the correctly localized Bud10p signal was seen as double rings in large budded cells or as single rings in newly divided cells (Fig. 5, B and C, cells 1–4). This correlation is consistent with the interpretation that a pulse of *BUD10* expression early in the cell cycle, just before bud emergence, established localized Bud10p, which was then maintained for the duration of the cell cycle.

Experiments were performed on synchronized cell cultures to test directly whether the appearance of a correctly localized signal was dependent on the cell cycle phase at which the pulse occurred, as suggested by the above experiments. Two inductions of *BUD10* expression were carried out: one pulse centered on late G1 and a second centered on S/G2 phase (Fig. 6 A). Of cells exhibiting a detectable Bud10p signal in the G1 induction experiment, a majority (65%) displayed correctly localized Bud10p with concentrations at the incipient bud sites of unbudded cells or at the small buds of newly budded cells (Fig. 6 B, cells 2 and 3). Some mislocalized signal (13%) was apparent after G1-centered induction; however, this signal was mostly found in medium-sized budded cells, apparently a result of imperfect synchrony (Fig. 6 B, cell 4). The remainder of the cells (22%) exhibiting Bud10p signal in intracellular compartments likely reflected the transit of Bud10p through the secretory pathway (Fig. 6 B, cell 1).

On induction of *BUD10* at the S/G2 phase, Bud10p was mislocalized throughout the plasma membrane of most cells (63%). In some cases Bud10p was seen concentrated at the tips of medium-sized buds (Fig. 6 C, cells 3 and 4). Bud tip localization was never seen in wild-type cells, suggesting that pulsed gene expression can create a novel localization pattern. A fraction of cells (25%) displayed a correctly localized Bud10p signal, but these cells were small budded, a result of imperfect synchrony. (Fig. 6 C, cell 2). This proportion (25%) corresponded very closely with the proportion of cells out of synchrony in this induction experiment (Fig. 6 A). 12% of cells exhibited Bud10p signal in intracellular compartments (Fig. 6 C, cell 1), just as observed above.

The results obtained from experiments performed on unsynchronized and synchronized cells demonstrate that correct localization of Bud10p can be restored in cells expressing *BUD10* under the *MET3* promoter. This correct localization is dependent on a pulse of *BUD10* expression taking place in late G1 phase.

Discussion

Genome-wide expression studies in yeast have demonstrated that the expression of a large fraction of genes is cell cycle regulated (Cho et al., 1998; Spellman et al., 1998). We sought to investigate the role of cell cycle–regulated gene expression in morphogenesis. Our study focused on *BUD3* and *BUD10*, two cell cycle–regulated genes involved in maintenance of the axial budding pattern in yeast. The phenotypes of these two genes and the subcellular localizations of their products have been well documented (Chant et al., 1995; Halme et al., 1996; Roemer et al., 1996). As such, *BUD3* and *BUD10* provide ideal candidates for cell cycle expression studies seeking to understand the importance of periodic expression to function.

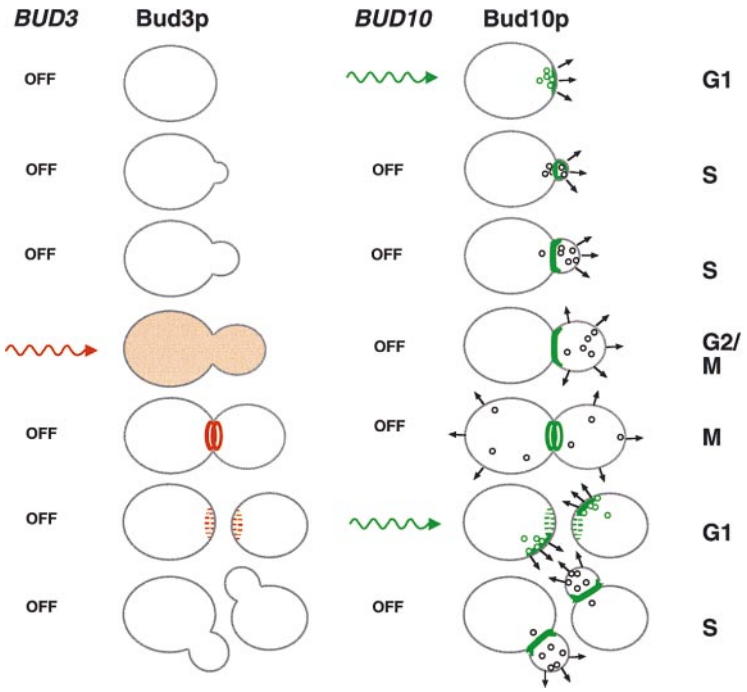

Figure 7. Proposed localization mechanisms of Bud3p and Bud10p. Cell cycle expression of *BUD3* leads to the production of cytoplasmic Bud3p (red), which localizes by diffusion and docking at the septin ring. *BUD10* is expressed in G1 at which time secretion is tightly focused on the nascent bud site. Bud10p (green) is delivered to the bud site and remains for the duration of the cell cycle in this position, which becomes the mother–bud neck.

Cell Cycle Regulation of BUD3 and BUD10 Transcription

Our observations argue strongly that regulated expression of *BUD3* and *BUD10* mRNAs is controlled principally at the level of transcription. This view was first suggested by analysis of the upstream sequences of *BUD3* and *BUD10*, which revealed elements predicted to be common promoter recognition sites for cell cycle–specific transcription factors. *BUD3* has been classed with a small group of genes expressed at G2, all of which possess a common upstream sequence speculated to mediate cell cycle regulated transcription (Spellman et al., 1998). The upstream sequence of *BUD10* contains three variant "Swi4/6-cell cycle-box" promoter elements, as well as one consensus and two variant "*MluI*-cell cycle-box" elements. Both elements are associated with genes expressed in late G1 (Koch and Nasmyth, 1994; Cho et al., 1998; Spellman et al., 1998).

The promoter-swap experiments confirmed experimentally that transcription is largely, if not entirely, responsible for the cell cycle periodicity of *BUD3* and *BUD10* mRNA expression. When placed under the control of the *MET3* promoter, the expression of both genes became cell cycle constitutive. Perhaps most convincing was the observation that placement of *BUD10* under the control of the *BUD3* promoter caused a pulse of *BUD10* mRNA expression to occur in S/G2, the period during which *BUD3* mRNA is normally expressed. These results confirmed that the regulation of *BUD3* and *BUD10* mRNA levels was dependent on cell cycle–specific transcription with the degradation of *BUD3* and *BUD10* mRNAs likely occurring constitutively throughout the cell cycle.

Regulated BUD3 Expression Determines the Timing of Bud3p Localization

Replacement of periodic *BUD3* expression in favor of uniform expression did not affect the function of Bud3p. Bud3p supported the axial budding pattern and localized to its correct position at the mother–bud neck. The only observed change was that Bud3p localized prematurely. We conclude that the temporal regulation of Bud3p localization to the mother–bud neck is driven by a rise in *BUD3* mRNA abundance and the corresponding rise in protein levels. It is known that Bud3p localization at the mother–bud neck depends upon the septin ring, which assembles at the incipient bud site and remains encircling the mother–bud neck for the remainder of the cell cycle (Byers and Goetsch, 1976; Haarer and Pringle, 1987; Ford and Pringle, 1991; Kim et al., 1991; Chant et al., 1995; Carroll et al., 1998; Mino et al., 1998). Therefore, it is not surprising that Bud3p is able to localize prematurely, since the septin ring is always present. These results are entirely consistent with a simple mechanism for Bud3p localization relying on direct, or indirect, affinity for the septin ring (Fig. 7). Accordingly, the temporal regulation of Bud3p localization observed in wild-type cells reflects the presence of Bud3p protein.

If Bud3p localizes normally to the mother–bud neck and supports axial budding when expressed constitutively, why is *BUD3* expression so tightly temporally regulated? One possibility is that S/G2-specific expression of *BUD3* prevents deleterious interactions with other factors. Overexpression of *BUD3* under the strong *GAL1* promoter led to cytokinesis defects in >40% of cells, defects reminiscent of a septin mutant phenotype. Interestingly, *BUD3* overexpression resulted in septin mislocalization as measured by the aberrant distribution of Cdc3p. Perhaps expression of *BUD3* during G1 permits Bud3p to interact with the septins during the time at which they are still assembling into the septin ring structure. Premature interaction could interfere with septin assembly. Similar but milder defects were observed when *BUD3* was expressed from the *MET3* promoter. Under normal expression conditions, such an effect, even minor, could confer a considerable selective disadvantage on cells.

Cell Cycle Regulated BUD10 Expression Directs the Localization of Its Product

Constitutive *BUD10* expression from the *MET3* promoter and delayed periodic expression from the *BUD3* promoter both affected Bud10p function. Cells displayed a reduction in the ability to direct the axial budding pattern, and Bud10p was not properly localized. In wild-type cells, Bud10p concentrates to the incipient bud site, in the mother–bud neck, and at the division sites of newly divided cells. Both alterations led to uniform distribution of Bud10p throughout the plasma membrane. Taken together, these results imply that a cell cycle–specific pulse of *BUD10* expression in late G1 is critical for Bud10p localization and subsequent function. To examine this hypothesis further, we artificially induced pulses of *BUD10* expression. An artificial pulse of *BUD10* expression around late G1 restored correct localization of Bud10p, whereas pulses of expression outside this time led to mislocalization of Bud10p throughout the plasma membrane.

Why is a pulse of *BUD10* expression in late G1 so critical to its localization? The most economical explanation for our observations is that establishment of the Bud10p localization pattern relies on the timing of its passage through the secretory pathway (Fig. 7). A pulse of Bud10p production in late G1 allows delivery of Bud10p via the secretory pathway during exactly the period when secretion is very tightly focused on the future bud site (Kilmartin and Adams, 1984; Lew and Reed, 1993). Once Bud10p is delivered to this location, the affinity of Bud10p for cell wall components or other bud-site factors retains Bud10p in this location for the duration of the cell cycle. As the bud grows outward, the position of the bud site becomes the mother–bud neck.

Three lines of evidence support this timed delivery hypothesis. First, all perturbations that caused *BUD10* expression outside of the late G1 window resulted in Bud10p mislocalization. Such observations make sense since during other phases of the cell cycle secretion is not directed to the bud site or the mother–bud neck (Lew and Reed, 1993). Second, correct localization of Bud10p was restored by creating an artificial pulse of *BUD10* expression in G1. Third, if the initial localization of Bud10p is dictated by the pattern of cell surface growth at the instant of *BUD10* expression, novel patterns of Bud10p localization should be produced by expression of *BUD10* in other windows of the cell cycle. This prediction was fulfilled: in the S/G2 centered pulse experiment, some cells exhibited a patch of Bud10p protein tightly localized to the bud tip (Fig. 6 C, cells 3 and 4). Such a localization pattern is presumably produced by expression of *BUD10* in a short window of the cell cycle when cell surface growth is directed to the bud tip. In addition to this evidence, it is well established that Bud10p is delivered to the cell surface via the secretory pathway (Halme et al., 1996; Roemer et al., 1996; Powers and Barlowe, 1998; Sanders et al., 1999).

Our hypothesis does not explain one aspect of Bud10p localization, the conversion of a loose concentration of Bud10p in the mother–bud neck to a tight double ring structure toward the end of the cell cycle. How this remodeling occurs remains unknown, though it likely involves Bud3p (Halme et al., 1996).

Despite the fact that altered timing of *BUD10* expression resulted in uniform membrane localization of Bud10p, half of the cells were able to maintain an axial pattern of budding. These results suggest the possibility that an interaction with a ligand found in the vicinity of the mother–bud junction allows Bud10p to be more active in generating a signal than the Bud10p in other locations. We support the notion that at least two levels of control produce the high degree of spatial specificity in Bud10p signaling: high local concentration, resulting from pulsed expression in combination with secretory targeting, and local activation of Bud10p, possibly through interaction with a ligand.

Do Pulses of Cell Cycle Expression Direct the Localization of Other Morphogenetic Factors?

The expression of several other genes involved in cellular morphogenesis are cell cycle regulated, including *BUD4*, *BUD8*, *BUD9*, and *RAX2*. Bud4p is a nonmembrane protein that acts in similar fashion to Bud3p. *BUD4* expression occurs at M phase (Cho et al., 1998; Spellman et al., 1998), and Bud4p forms rings encircling the mother–bud neck in a septin-dependent manner (Sanders and Herskowitz, 1996). Interestingly, the *BUD4* promoter shares sequence similarity to those of *BUD3* and *CLB2* (Sanders and Herskowitz, 1996), and all three promoters contain a putative Fkh1p-binding site (Zhu et al., 2000). We consider it likely that the pulse of *BUD4* expression controls the timing of its localization to the mother–bud neck, as observed for Bud3p.

Three genes required for the bipolar budding pattern, *BUD8*, *BUD9*, and *RAX2* (Zahner et al., 1996; Chen et al., 2000) are also expressed periodically in the cell cycle (Cho et al., 1998; Spellman et al., 1998). Like Bud10p, the products of *BUD8*, *BUD9*, and *RAX2* are membrane proteins; therefore, timing of expression could play a large part in directing the localizations of these morphogenetic marker proteins as well. Finally, a very recent report suggests that the localization of Crh1p, a secreted cell wall protein, is determined by the cell cycle timing of *CRH1* expression (Rodríguez-Peña et al., 2000).

The Importance of Timed Gene Expression and Cell Cycle Regulation

Given the prevalence of cell cycle–dependent transcription in yeast, it seems likely that periodic transcription will serve as a general mechanism of regulation within the cell cycle. In very few instances has the importance of the periodic expression been directly tested. DNA replication is dependent on the late G1 expression of *CLB5* and *CLB6* (Epstein and Cross, 1992; Schwob and Nasmyth, 1993), and it is thought that the specific timing of expression of these cyclins is critical. Indeed, the inappropriate expression of *CLB2*, encoding a mitotic cyclin, interferes with the initiation of DNA replication (Detweiler and Li, 1998). In addition, the initiation factor Cdc6p must be synthesized in G1 to control the initiation of DNA replication effectively (Piatti et al., 1996). Beyond these studies and those presented here, it shall be of interest to learn precisely the role of cell cycle–specific transcription in diverse aspects of cellular function now that we know the cell cycle expression profile of every yeast gene (Cho et al., 1998; Spellman et al., 1998).

Conclusion

We have examined the importance of timed gene expression in cellular morphogenesis in two test cases. For Bud10p, a secreted protein, the timing of *BUD10* expression played a major role in directing its localization. In principle, pulsed gene expression may direct the localization of any secreted protein in a cell type that has spatially regulated patterns of cell surface growth.

A localization mechanism that relies on the delivery of a protein through the secretory pathway, rather than specific affinity for a docking site, affords a high degree of flexibility in changing patterns of protein localization within cells. Changes in the timing of expression would allow for the evolution of a novel protein localization pattern without structural changes in the protein. In the case of cells that must frequently remodel, a secretory targeting mechanism of protein localization could allow tremendous plasticity in altering cellular architecture such as occurs during changes in synaptic connectivity in neurons.

We are very grateful to Laura Schenkman, John Pringle, and members of the Chant lab for helpful discussions. We thank Ben Benton for providing the *cdc15-2*^{ts} strain, Erica Johnson for the *CDC3-HA* strain, Erfei Bi for an unpublished *GAL* induction plasmid, and the reviewers for their critical and helpful comments on the manuscript.

M. Lord is supported by a Human Frontiers Science Program Organization long-term fellowship. Work in J. Chant's laboratory is supported by a National Institutes of Health grant (GM49782).

Submitted: 30 June 2000
Revised: 31 October 2000
Accepted: 31 October 2000

References

Bender, A., and J.R. Pringle. 1989. Multicopy suppression of the cdc24 budding defect in yeast by *CDC42* and three newly identified genes including the ras-related *RSR1*. *Proc. Natl. Acad. Sci. USA.* 86:9976–9980.

Benton, B.K., A. Tinkelenberg, I. Gonzalez, and F.R. Cross. 1997. Cla4p, a *Saccharomyces cerevisiae* Cdc42p-activated kinase involved in cytokinesis, is activated at mitosis. *Mol. Cell. Biol.* 17:5067–5076.

Byers, B., and L. Goetsch. 1976. A highly ordered ring of membrane-associated filaments in budding yeast. *J. Cell. Biol.* 69:717–721.

Carroll, C.W., R. Altman, D. Schieltz, J.R. Yates, and D. Kellogg. 1998. The septins are required for the mitosis-specific activation of the Gin4 kinase. *J. Cell Biol.* 143:709–717.

Chant, J., and I. Herskowitz. 1991. Genetic control of bud site selection in yeast by a set of gene products that constitute a morphogenetic pathway. *Cell.* 65: 1203–1212.

Chant, J., and J.R. Pringle. 1995. Patterns of bud-site selection in the yeast *Saccharomyces cerevisiae*. *J. Cell Biol.* 129:751–765.

Chant, J., K. Corrado, J.R. Pringle, and I. Herskowitz. 1991. Yeast *BUD5*, encoding a putative GDP-GTP exchange factor, is necessary for bud site selection and interacts with bud formation gene *BEM1*. *Cell.* 65:1213–1224.

Chant, J., M. Mischke, E. Mitchell, I. Herskowitz, and J.R. Pringle. 1995. Role of Bud3p in producing the axial budding pattern of yeast. *J. Cell Biol*. 129: 767–778.

Chen, T., T. Hiroko, A. Chaudhuri, F. Inose, M. Lord, S. Tanaka, J. Chant, and A. Fujita. 2000. Multigenerational cortical inheritance of the Rax2 protein in orienting polarity and division in yeast. *Science*. In press.

Cho, R.J., M.J Campbell, E.A. Winzeler, L. Steinmetz, A. Conway, L. Wodicka, T.G. Wolfsberg, A.E. Gabrielian, D. Landsman, D.J. Lockhart, and R.W. Davis. 1998. A genome-wide transcriptional analysis of the mitotic cell cycle. *Mol. Cell.* 2:65–73.

Chu, S., J. DeRisi, M. Eisen, J. Mulholland, D. Botstein, P.O. Brown, and I. Herskowitz. 1998. The transcriptional program of sporulation in yeast. *Science.* 282:699–705.

Detweiler, C.S., and J.J. Li. 1998. Ectopic induction of Clb2 in early G1 phase is sufficient to block prereplicative complex formation in *Saccharomyces cerevisiae. Proc. Natl. Acad. Sci. USA*. 95:2384–2389.

Epp, J.A., and J. Chant. 1997. An IQGAP-related protein controls actin-ring formation and cytokinesis in yeast. *Curr. Biol.* 7:921–929.

Epstein, C.B. and F.R. Cross. 1992. *CLB5*: a novel B cyclin from budding yeast with a role in S phase. *Genes Dev*. 6:1695–1706.

Field, J., J. Nikawa, D. Broek, B. MacDonald, L. Rodgers, I.A. Wilson, R.A. Lerner, and M. Wigler. 1988. Purification of a RAS-responsive adenylyl cyclase complex from *Saccharomyces cerevisiae* by use of an epitope addition method. *Mol. Cell. Biol.* 8:2159–2165.

Ford, S.K., and J.R. Pringle. 1991. Cellular morphogenesis in the *Saccharomyces cerevisiae* cell cycle: localization of the *CDC11* gene product and the timing of events at the budding site. *Dev. Genet.* 12:281–292.

Freifelder, D. 1960. Bud position in *Saccharomyces cerevisiae*. *J. Bacteriol*. 80: 567–568.

Fujita, A., C. Oka, Y. Arikawa, T. Katagari, A. Tonrichi, S. Kuhara, and Y. Misumi. 1994. A yeast gene necessary for bud site selection encodes a protein similar to insulin degrading enzymes. *Nature.* 372:567–570.

Haarer, B.K., and J.R. Pringle. 1987. Immunofluorescence localization of the *Saccharomyces cerevisiae CDC12* gene product to the vicinity of the 10-nm filaments in the mother–bud neck. *Mol. Cell. Biol*. 7:3678–3687.

Halme, A., M. Michelitch, E.L. Mitchell, and J. Chant. 1996. Bud10p directs axial cell polarization in budding yeast and resembles a transmembrane receptor. *Curr. Biol*. 6:570–579.

Hicks, J.B., J.N. Stathern, and I. Herskowitz. 1977. Interconversion of yeast mating types. III. Action of homothallism (*HO*) gene in cells homozygous for the mating type locus. *Genetics*. 85:373–393.

Johnson, E.S., and G. Blobel. 1999. Cell cycle–regulated attachment of the ubiquitin-related protein SUMO to the yeast septins. *J. Cell Biol.* 147:981–993.

Kilmartin, J.V., and A.E.M. Adams. 1984. Structural rearrangements of tubulin and actin during the cell cycle of the yeast *Saccharomyces*. *J. Cell Biol.* 98: 922–933.

Kim, H.B., B.K. Haarer, and J.R. Pringle. 1991. Cellular morphogenesis in the *Saccharomyces cerevisiae* cell cycle: localization of the *CDC3* gene product and the timing of events at the budding site. *J. Cell. Biol.* 112:535–544.

Koch, C., and K. Nasmyth. 1994. Cell cycle regulated transcription in yeast. *Curr. Opin. Cell Biol.* 6:451–459.

Köhrer, K., and H. Domdey. 1991. Preparation of high molecular weight RNA. *Methods Enzymol.* 194:398–405.

Lew, D.J., and S.I. Reed. 1993. Morphogenesis in the yeast cell cycle: regulation by Cdc28 and cyclins. *J. Cell Biol.* 120:1305–1320.

Longtine, M.S., D.J. DeMarini, M.L. Valencik, O.S. Al-Awar, H. Fares, C. De Virgilio, and J.R. Pringle. 1996. The septins: roles in cytokinesis and other processes. *Cur. Opin. Cell Biol.* 8:106–119.

Mino, A., K. Tanaka, T. Kamei, M. Umikawa, T. Fujiwara, and Y. Takai. 1998. Shs1p: a novel member of septin that interacts with Spa2p, involved in polarized growth in *Saccharomyces cerevisiae*. *Biochem. Biophys. Res. Commun.* 251:732–736.

Piatti S., T. Bohm, J.H. Cocker, J.F. Diffley, and K. Nasmyth. 1996. Activation of S-phase-promoting CDKs in late G1 defines a "point of no return" after which Cdc6 synthesis cannot promote DNA replication in yeast. *Genes Dev*. 10:1516–1531.

Powers, J., and C. Barlowe. 1998. Transport of Axl2p depends on Erv14p, an ER-vesicle protein related to the *Drosophila cornichon* gene product. *J. Cell Biol.* 142:1209–1222.

Pringle, J.R. 1991. Staining of bud scars and other cell wall chitin with calcofluor. *Methods Enzymol.* 194:732–735.

Pringle, J.R., A.E.M. Adams, D.G. Drubin, and B.K. Haarer. 1991. Immunofluorescence methods for yeast. *Methods Enzymol.* 194:565–602.

Rodríguez-Peña, J.M., V.J. Cid, J. Arroyo, and C. Nombela. 2000. A novel family of cell wall-related proteins regulated differently during the yeast life cycle. *Mol. Cell. Biol*. 20:3245–3255.

Roemer, T., D. Madden, J. Chang, and M. Snyder. 1996. Selection of axial growth sites in yeast requires Axl2p, a novel plasma membrane glycoprotein. *Genes Dev*. 10:777–793.

Rose, M.D., F. Winston, and P. Hieter. 1990. Methods in yeast genetics. Cold Spring Harbor Laboratory Press, Cold Spring Harbor, NY. 123 pp.

Sambrook, J., E.F. Fritsch, and T. Maniatis. 1989. Molecular Cloning: A Laboratory Manual. Cold Spring Harbor Laboratory Press, Cold Spring Harbor, NY.

Sanders, S.L., and I. Herskowitz. 1996. The Bud4 protein of yeast, required for axial budding, is localized to the mother/bud neck in a cell cycle–dependent manner. *J. Cell Biol.* 134:413–427.

Sanders, S.L., M. Gentzsch, W. Tanner, and I. Herskowitz. 1999. *O*-Glycosylation of Axl2/Bud10p by Pmt4p is required for its stability, localization, and function in daughter cells. *J. Cell Biol.* 145:1177–1188.

Schwob, E., and K. Nasmyth. 1993. *CLB5* and *CLB6*, a new pair of B cyclins involved in DNA replication in *Saccharomyces cerevisiae. Genes Dev*. 7:1160–1175.

Spellman, P.T., G. Sherlock, M.Q. Zhang, V.R. Iyer, K. Anders, M.B. Eisen, P.O. Brown, D. Botstein, and B. Futcher. 1998. Comprehensive identification of cell cycle-regulated genes of the yeast *Saccharomyces cerevisiae* by microarray hybridization. *Mol. Biol. Cell.* 9:3273–3297.

Zahner, J.E., H.A. Harkins, and J.R. Pringle. 1996. Genetic analysis of the bipolar pattern of bud site selection in the yeast *Saccharomyces cerevisiae*. *Mol. Cell. Biol.* 16:1857–1870.

Zhu, G., P.T. Spellman, T. Volpe, P.O. Brown, D. Botstein, T.N. Davis, and B. Futcher. 2000. Two yeast forkhead genes regulate the cell cycle and pseudohyphal growth. *Nature*. 406:90–94.